Vegetation optical depth retrieval from AMSR-E/AMSR2 observations using L-MEB inversion

Mengjia Wang, Jean-Pierre Wigneron, Rui Sun, Philippe Ciais, Martin Brandt, Yi Liu, Frédéric Frappart, Xiaojun Li, Xiangzhuo Liu, Lei Fan, et al.

VEGETATION OPTICAL DEPTH RETRIEVAL FROM AMSR-E/AMSR2 OBSERVATIONS USING L-MEB INVERSION

Mengjia Wang[1,2,3], *Jean-Pierre Wigneron*[3*], *Rui Sun*[1,2*], *Philippe Ciais* [4], *Martin Brandt* [5], *Yi Liu*[6] ,*Frédéric Frappart* [7,8], *Xiaojun Li* [3], *Xiangzhuo Liu* [3], *Lei Fan* [6], *Rasmus Fensholt* [5]

1. State Key Laboratory of Remote Sensing Science, Faculty of Geographical Science, Beijing Normal University, Beijing 100875, China; 2. Beijing Engineering Research Center for Global Land Remote Sensing Products, Faculty of Geographical Science, Beijing Normal University, Beijing 100875, China; 3. INRAE, UMR1391 ISPA, F-33140, Villenave d'Ornon, France; 4. Laboratoire des Sciences du Climat et de l'Environnement, CEA/CNRS/UVSQ/Université Paris Saclay, Gif-sur-Yvette, France; 5. Department of Geosciences and Natural Resource Management, University of Copenhagen, Copenhagen, Denmark; 6. School of Geographical Sciences, Nanjing University of Information Science and Technology, Nanjing, China; 7. Laboratoire d'Etudes en Géophysique et Océanographie Spatiales (LEGOS), 31400 Toulouse, French ; 8. Géosciences Environnement Toulouse (GET), 31400 Toulouse, France.

*Corresponding authors: Jean-Pierre Wigneron, Rui Sun;

E-mail address: jean-pierre.wigneron@inrae.fr, sunrui@bnu.edu.cn.

ABSTRACT

Decade years of efforts on the retrieval of soil moisture based on radiative transfer model have largely improved the accuracy of soil moisture (SM). This paper focus on the other parameter, namely vegetation optical depth (VOD). We retrieved X-band VOD from AMSR-E and AMSR2 observations by inverting the L-MEB model (Wigneron et al. 2007 [1]) at X-band, considering that SM was known. As SM input to the L-MEB inversion we used the ECMWF SM product. This step avoids correlation between VOD and SM retrievals from the mono-angular AMSR-E observations. In a first step we evaluated the retrieved VOD with the Copernicus Global Land Service (CGLS) LAI. The evaluation results indicate our model has a great potential for VOD retrievals from AMSR-E/2 satellite data.

INTRODUCTION

In recent years, much attention has been placed on the role of terrestrial biosphere dynamics in the climate system. Brandt et al. [2] found there is a strong linear correlation with no clear sign of saturation, even in densely vegetated areas, between SMOS L-VOD based on L-MEB model and aboveground vegetation carbon stocks among different land cover classes. However, SMOS monitored the Earth since 2010 limiting our capability to evaluate long-term global carbon changes, such as over several decades. Therefore, there is a need to extend the application of the L-MEB model to other satellite data, such as AMSR-E/2.

Over the last decade, lots of efforts have been put on the retrieval of soil moisture for which the accuracy was greatly improved. For more than a decade, the European Centre for Medium-Range Weather Forecasts (ECMWF) has used in-situ and remote sensing observations to operationally constrain the temporal evolution of soil moisture[3]. In this paper, we assume ECMWF SM is accurate enough to be used as an input to the L-MEB model (a more accurate name for the model would be X-MEB, but we used "L-MEB" which is a more standard name). We used an iterative optimization procedure to retrieve VOD, the initial (or first guess) value of VOD is the yearly average LPRM VOD.

L-MEB MODEL

In the L-MEB model, the simulation of the land surface emission is based on the τ-ω radiative transfer model using simplified (zero-order) radiative transfer equations. The upwelling radiation (brightness temperature) as observed from above the canopy consists of three components: 1) the radiation from the soil layer attenuated by the overlaying vegetation; 2) the upward radiation from the vegetation; and 3) the downward radiation from the vegetation, reflected upwards by the soil layer and again attenuated by the vegetation as given in the following equation [4, 5]:

$$T_b^P = T_S\Gamma(\theta)e_r + (1-\omega)\big(1-\Gamma(\theta)\big)T_C + (1-\omega)\big(1-\Gamma(\theta)\big)(1 - e_r)\Gamma(\theta)T_C$$

where P is the polarization, we only used horizontal polarization in this paper; T_S and T_C are the temperatures of the soil and the canopy respectively; e_r is the soil emissivity determined by soil moisture, temperature and roughness; ω is the effective scattering albedo; Γ is the vegetation transmissivity determined by VOD (dimensionless) and the observing incidence angle (θ) as given in the following equation:

$$\Gamma = \exp\left(\frac{-VOD}{\cos(\theta)}\right)$$

In this paper, we assume ECMWF SM is accurate enough to be used as a known input to the L-MEB model, therefore, VOD becomes the only unknown parameter. The approach of retrieving VOD is to minimize the following cost function:

$$\text{cost function} = \frac{\sum_{i=1}^{2}(TB_p(\theta)_{obs} - TB_p(\theta)_{sim})^2}{\sigma(\mathrm{TB})^2} + \frac{(\mathrm{VOD}_{ini} - \mathrm{VOD})^2}{\sigma(\mathrm{VOD})^2}$$

where VOD_{ini} denotes the initial VOD equal to the yearly average of the LPRM VOD, $\sigma(\mathrm{VOD})$ is set as a constant value of 0.5.

Previous studies have shown that the brightness temperature is sensitive to the soil roughness (HR)[6] and the effective vegetation scattering albedo (ω) [7]. In other words, the quality of the retrieved VOD could be affected by the values of these two parameters. By now, we have only completed the calibration of ω. We first set HR equal to 0, and change the value of ω from 0 to 0.08. Consequently, the retrieved VOD in this study does not only reflect the vegetation information, it also incorporates the surface roughness effects. In order to save the time of the calibration process, we started with the African continent where various vegetation classes are included. In a first step, we assumed CGLS LAI is a good proxy of the VOD. So the optimum ω is the one that lead to the best temporal correlation between the retrieved VOD and the CGLS LAI.

DATA

AMSR-2, launched on 18 May 2012 on board the JAXA GCOMW1 satellite, provides the global measurements of vertically (V) and horizontally (H) polarized microwave emissions at six frequencies (6.9, 10.7, 18.7, 23.8, 36.5, 89.0 GHz) with descending and ascending orbital equatorial crossings at 01:30 and 13:30 local time. In this first analysis, we focused on X-band (10.7GHz), horizontal polarization, descending data for only one year of 2016. The ECMWF dataset used in this study for the VOD retrieval is based on the ERA-Interim dataset which used a numerical weather prediction (NWP) system (IFS-Cy31r2) to produce the reanalyzed data. The ECMWF soil surface (Level 1, top 0–7 cm soil layer) and soil deep temperature (Level 3, 28-100 cm) were used to compute the effective soil temperature. The surface (Level 1) soil moisture was chosen as a known input to the model. The 10-day LAI product used in this study is obtained from the CGLS website (https://land.copernicus.eu/global/). LPRM X-VOD[8], CCI X-VOD [9] and LPDR X-VOD [10] were downloaded, respectively, from Goddard Earth Sciences Data and Information Services Center (GES DISC), Vegetation Optical Depth Climate Archive (VODCA) and National Snow and Ice Data Center (NSIDC). These three products are calculated using an iterative solution of the radiative transfer equations to retrieve VOD and soil moisture at the same time from vertical and horizontal polarized microwave data.

RESULT

By now, we have only completed the calibration of ω. We first set HR equal to 0 and change the value of ω ranging from 0 to 0.08. Therefore, the retrieved VOD in this study doesn't only reflect the vegetation information, also incorporates the surface roughness effects. We evaluated the retrieved VOD against the CGLS LAI, and only the temporal correlation was considered in this study. Table 1 shows the percentages accounting for which the specific model produced the highest temporal correlation for different effective scattering albedo values. It's clear that LMEB produced the largest number of pixels with highest temporal correlation for most of the tested effective scattering albedo values (0 to 0.06). Then LPDR is the second model producing the highest temporal correlation. On the contrary, CCI and LPRM only have a small fraction pixels showing highest temporal correlation, less than 20% and 10 % respectively. For LMEB model, the proportion fell down from 61.35% to 27.30% when increasing ω from 0 to 0.08.

Table1. The percentage of pixels for the specific model producing the highest temporal correlation

ω	LMEB	LPDR	CCI	LPRM
0	0.6135	0.2652	0.0796	0.0417
0.01	0.5916	0.2762	0.0870	0.0453
0.02	0.5588	0.2912	0.0989	0.0511
0.03	0.5298	0.3060	0.1069	0.0573
0.04	0.4898	0.3227	0.1212	0.0663
0.06	0.4233	0.3487	0.1482	0.0798
0.08	0.2730	0.4236	0.2055	0.0979

(Red presents the high values, on the contrary, green presents the low values).

Regarding the above study, we fixed the optimum parameters (HR = 0 and ω = 0). Figure 1 (left) illustrates the distribution of the model which produced the highest temporal correlation. It is easy to find that LMEB owned the largest proportion of pixels (61.35%) with the highest temporal correlation with the CGLS LAI， especially in the west of the Africa. LPDR surpassed the other models over a fraction of 26.52% of the pixels which were mainly located in the east and the south of the Africa. In comparison to the former 2 models, CCI and LPRM showed only a few pixels (less than 10%) with the highest temporal correlation.

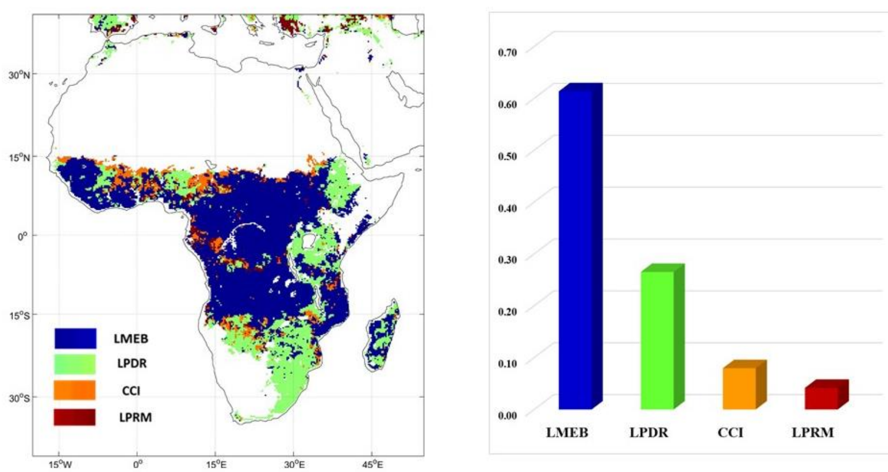

Figure 1. Left: the distribution of the model which produced the highest temporal correlation; right: the histogram of the percentage for each model with the highest temporal correlation.

CONCLUSION

We evaluated a new retrieval approach of AMSR-E/2 X-VOD using the L-MEB model. In this study, we assumed ECMWF SM as a known input to the L-MEB inversion and we only retrieved VOD. In this study, we first set HR equal to 0, and tested 7 values of the effective vegetation scattering albedo (ω) from 0 to 0.08. We evaluated the retrieved VOD with the CGLS LAI by comparing the temporal correlation with other VOD products. For most of the tested ω values (from 0 to 0.06), LMEB surpassed other models by producing the highest temporal correlation over the largest fraction of pixels (60 % of the studied area in Africa). This model showed best performance in the west of the Africa, then followed by LPDR especially in the east and the south of the Africa. Future studies will extend the analysis to a combined calibration of both ω and HR, and to the spatial correlation with biomass, NDVI and LAI.

ACKNOWLEDGMENT

This work was jointly supported by the National Key R&D Program of China (2017YFA0603002, 2016YFB0501502), CSC funding and the TOSCA (Terre Océan Surfaces Continentales et Atmosphère) CNES (Centre National d'Etudes Spatiales) programme.

REFERENCES

[1] J. P. Wigneron *et al.*, "L-band Microwave Emission of the Biosphere (L-MEB) Model: Description and calibration against experimental data sets over crop fields," *Remote Sensing of Environment,* vol. 107, no. 4, pp. 639-655, 2007.

[2] M. Brandt *et al.*, "Satellite passive microwaves reveal recent climate-induced carbon losses in African drylands," *Nat Ecol Evol,* vol. 2, no. 5, pp. 827-835, May 2018.

[3] J. Muñoz-Sabater, "Incorporation of Passive Microwave Brightness Temperatures in the ECMWF Soil Moisture Analysis," *Remote Sensing,* vol. 7, no. 5, pp. 5758-5784, 2015.

[4] R. Fernandez-Moran *et al.*, "SMOS-IC: An Alternative SMOS Soil Moisture and Vegetation Optical Depth Product," *Remote Sensing,* vol. 9, no. 5, 2017.

[5] X. Li *et al.*, "Compared performances of SMOS-IC soil moisture and vegetation optical depth retrievals based on Tau-Omega and Two-Stream microwave emission models," *Remote Sensing of Environment,* vol. 236, 2020.

[6] L. Karthikeyan *et al.*, "Simultaneous retrieval of global scale Vegetation Optical Depth, surface roughness, and soil moisture using X-band AMSR-E observations," *Remote Sensing of Environment,* vol. 234, 2019.

[7] M. Parrens *et al.*, "Estimation of the L-Band Effective Scattering Albedo of Tropical Forests Using SMOS Observations," *IEEE Geoscience and Remote Sensing Letters,* vol. 14, no. 8, pp. 1223-1227, 2017.

[8] M. Owe, R. de Jeu, and T. Holmes, "Multisensor historical climatology of satellite-derived global land surface moisture," *Journal of Geophysical Research,* vol. 113, no. F1, 2008.

[9] J. Du, J. S. Kimball, L. A. Jones, Y. Kim, J. Glassy, and J. D. Watts, "A global satellite environmental data record derived from AMSR-E and AMSR2 microwave Earth observations," *Earth System Science Data,* vol. 9, no. 2, pp. 791-808, 2017.

[10] L. Moesinger *et al.*, "The Global Long-term Microwave Vegetation Optical Depth Climate Archive VODCA," *Earth System Science Data Discussions,* pp. 1-26, 2019.